Coercivity mechanisms in positive exchange-biased Co films and Co/Pt multilayers

T. L. Kirk,[1,2] O. Hellwig,[1] and Eric E. Fullerton[1]
[1]*IBM Almaden Research Center, 650 Harry Road, San Jose, California 95120*
[2]*Department of Physics, University of California–San Diego, La Jolla, California 92093-0319*
(Received 8 February 2002; published 10 June 2002)

We describe magnetization measurements on a simple model system that mimics the behavior of positive exchange bias. The system consists of an antiferromagnetic CoO layer exchange coupled to antiferromagnetically coupled Co/Ru/Co or $[Co/Pt]_N/Co/Ru/[Co/Pt]_M$ multilayer films with in-plane and out-of-plane anisotropy, respectively. In both cases, the two ferromagnetic layers were chosen to have different thickness with the thinner layer coupled to the CoO layer. When cooled below the blocking temperature of the CoO layer the thinner ferromagnetic layer is pinned and the low-field response is governed by the reversal of the thicker ferromagnetic layer with an effective exchange bias that is mediated via the Ru interlayer. For all the films studied we observe a transition in the effective bias from negative to positive with increasing cooling field. However, when varying the cooling field we find three distinct coercivity behaviors during the transition from positive to negative bias that depends on the anisotropy and microstructure of the ferromagnetic layers.

DOI: 10.1103/PhysRevB.65.224426 PACS number(s): 75.60.−d, 75.50.Ee, 75.70.Cn

I. INTRODUCTION

When a ferromagnetic (FM) thin film in contact with an antiferromagnetic (AFM) thin film is cooled through the Néel temperature (T_N) of the AFM layer in an applied magnetic field, the hysteresis loop of the FM often develops a loop shift (or bias) and an enhanced coercivity.[1–3] These exchange-anisotropy effects arise as the spin order of the AFM is established in the presence of the FM via the interfacial FM-AFM exchange interaction. Control over the exchange-bias field (H_{EB}) and coercivity (H_C) has many technological applications, such as suppressing domain formation and biasing magnetic devices.[4,5] Theorists have used these two macroscopic quantities, H_{EB} and H_C to create models that provide a microscopic understanding of the exchange biasing.[6,7] However, a general theory is still lacking. Towards a more fundamental understanding of the bias process recent studies have exploited double superlattice structures to mimic AFM/FM bilayer structures.[8–10] In such structures, the magnetic interactions can be controlled and tuned in the thin-film deposition process.

In general it has been found that cooling in a positive applied field results in a shift of the hysteresis loop towards negative exchange fields H_{EB} or negative bias. However, recent experiments have discovered a new and rather surprising phenomenon of positive exchange bias in FeF_2/Fe and MnF_2/Fe bilayers.[11–15] For certain structures it was observed that for ''small'' external cooling fields, the samples exhibited the expected negative bias. However, for large cooling fields the samples became positively biased. In addition, it was observed that the coercivity of the Fe layer was dependent on the magnitude of the cooling field with the coercivity reaching a maximum for intermediate external cooling field that roughly corresponded to where the bias changed from negative to positive.[15] Positive biasing has been related to models where the surface spins of the AFM layer are antiferromagnetically coupled to the FM layer.[11,12,15,16] The biasing process is then determined by a competition between the Zeeman energy acting on the surface spins of the AFM and the antiferromagnetic exchange interaction between the FM and AFM layer. That is, for small fields the AFM surface spin orientation is determined by the exchange interaction with the FM and is antiparallel to the field-cooling direction. However, for large cooling fields the applied field overcomes the interfacial interaction and aligns the AFM surface spins parallel to the field and explains the change in bias direction with increasing cooling field magnitude. Positive bias has also been observed for ferromagnetic FeSn layers that are antiferromagnetically coupled to ferrimagnetic FeGd layers[17] supporting this model. The anomalous coercivity behavior was understood as arising from spin-frustration at the AFM-FM interface.[15]

In the present manuscript we describe magnetization measurements on a simple model system that mimics the behavior of positive exchange bias. The system consists of an AFM CoO layer exchange coupled to either an antiferromagnetically coupled Co/Ru/Co trilayer with planar anisotropy or antiferromagnetically coupled $[Co/Pt]_N/Co/Ru/[Co/Pt]_M$ multilayers with perpendicular anisotropy. In these structures the FM layer next to the CoO is kept thinner than the second FM layer to mimic the surface spins of the AFM layer. When cooled below the blocking temperature of the CoO layer the thinner FM layer is pinned and the low-field response is governed by the reversal of the thicker FM layer. In this case the effective exchange bias is mediated to the thicker FM layer via the Ru interlayer. These structures are similar to the double superlattice structures where interlayer coupling is used to modulate the exchange-bias interaction.[8–10] However, for the double superlattices the magnetization is not field cooled but is set by large applied fields and only negative bias is observed independent of the sign of the interlayer coupling.[10] For the present structures cooling in small applied fields results in negative exchange bias while cooling in large fields gives an effective positive bias. By measuring the cooling field dependence of the exchange bias and coercivity of the thicker FM layer, the role of the anisotropy and disorder on positive bias can be investigated in detail. For all the films studied we observe a transition from negative to posi-

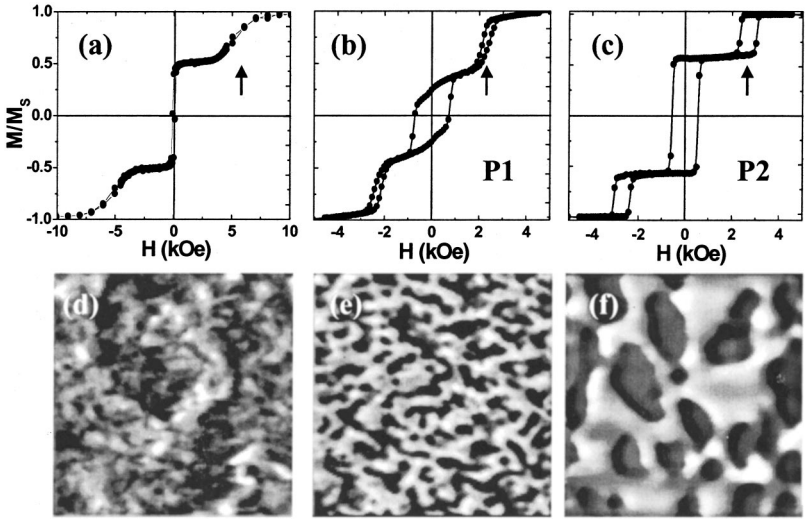

FIG. 1. Room-temperature hysteresis loops (a)–(c) and MFM images (d)–(f) for antiferromagnetically coupled longitudinally magnetized Co/Ru/Co trilayer (a) and (d) and for the perpendicularly magnetized $[\mathrm{Co/Pt}]_N/\mathrm{Co/Ru/}[\mathrm{Co/Pt}]_M$ samples $P1$ (b) and (e) and $P2$ (c) and (f). The hysteresis loop in (a) was measured with an in-plane applied field while (b) and (c) were measured with a perpendicular applied field. The arrows in (a)–(c) indicate the exchange field H_{ex} where the thinner FM layer reverses its magnetization direction. The MFM images were measured in remanence after demagnetizing the sample and the image scale is $5\times5\ \mu\mathrm{m}^2$.

tive bias with increasing cooling field. However, we find three distinct behaviors for the cooling-field dependence of the coercivity at this transition. For the Co/Ru/Co samples with planar anisotropy we observe a suppression of the coercivity of the thicker FM layer. For the perpendicular multilayers we observe either an enhancement of the coercivity or a bifurcation of the hysteresis loop when the cooling field is tuned to the transition region from negative to positive bias. The coercivity enhancement is in close agreement to that observed for $MnFe_2/Fe$ bilayers.[15]

II. EXPERIMENTAL PROCEDURE

The films were dc magnetron sputtered in a 3 mTorr Ar atmosphere onto Si_3N_X-coated Si (100) substrates at room temperature. The base pressure was $<5\times10^{-8}$ Torr prior to deposition. The substrates were rotated at $\sim$2 Hz during deposition to ensure film uniformity. Each film was grown onto a 200-Å Pt buffer. The in-plane anisotropy structures studied were Co(40 Å)/Ru(9 Å)/Co (16 Å)/CoO ($\sim$10 Å). The Ru thickness was tuned to optimize the antiferromagnetic interlayer coupling. The Co/CoO bilayer was formed by depositing a 22-Å Co layer that was allowed to oxidize in atmosphere such that 6–7 Å of the Co was transformed into $\sim$10 Å of CoO.[18]

The out-of-plane anisotropy samples were made in two different ways. The first structure is $[\mathrm{Pt}(7\ \text{Å})/\mathrm{Co}(4\ \text{Å})]_{10}/\mathrm{Ru}(9\ \text{Å})/[\mathrm{Co}(4\ \text{Å})/\mathrm{Pt}(7\ \text{Å})]_2/\mathrm{Co}(10\ \text{Å})/\mathrm{CoO}(10\ \text{Å})$. The Co/CoO again was formed by oxidizing a 17-Å Co layer. For the second structure the CoO was formed directly on the Pt buffer layer by oxidizing a 7-Å Co layer. The antiferromagnetically coupled multilayer was subsequently grown onto the CoO layer. The final structure we obtained was $\mathrm{CoO}(10\ \text{Å})/[\mathrm{Co}(4\ \text{Å})/\mathrm{Pt}(7\ \text{Å})]_2/\mathrm{Co}(4\ \text{Å})/\mathrm{Ru}(9\ \text{Å})/[\mathrm{Co}(4\ \text{Å})/\mathrm{Pt}(7\ \text{Å})]_{10}$. We will refer to these two perpendicular anisotropy structures as $P1$ and $P2$, respectively. For all structures, the Co layers grow (111) textured such that the CoO is similarly textured and forms AFM domains where the spins have out-of-plane as well as in-plane projections. This allows the CoO layer to bias structures that have either in-plane or perpendicular magnetization.[18]

The room-temperature magnetic properties were characterized using a 5-T Quantum Design SQUID magnetometer, polar magneto-optic Kerr effect (MOKE) magnetometer and a magnetic force microscope (MFM). The low-temperature magnetic properties were measured using the SQUID magnetometer. The full temperature dependence of the samples was measured but we will report on the room temperature and 50 K results that highlight the physics of interest.

III. EXPERIMENT RESULTS

A. Room temperature

Figures 1(a)–1(c) show the room temperature *M-H* loops of the three samples. At room temperature the CoO layer is nonmagnetic and does not influence the system. Figure 1(a) is measured with an in-plane field while Figs. 1(b) and 1(c) are measured perpendicular to the film. All three samples show the characteristic behavior of antiferromagnetically coupled trilayers.[19] For large fields the interlayer coupling is overcome and the layers are parallel to the field. As the field is reduced the interlayer coupling overcomes the applied field and the thinner FM layer reverses at the exchange fields H_{ex} that are identified by the arrows in Fig. 1. From this field we can estimate the interlayer exchange coupling J_{ex} of $\sim$0.5 ergs/cm^2 for these samples via $J_{\mathrm{ex}}\sim H_{\mathrm{ex}}\ M_S\ t$ where M_S and t are the magnetization and thickness of the thinner FM layer, respectively.[19] For each sample the remenant state is with the adjacent magnetizations antiparallel and the thicker layer parallel to the previously applied field direction. There are clear differences in the magnetic behavior of the perpendicular samples $P1$ and $P2$. Sample $P2$ exhibits discrete jumps in the magnetization reversal indicating correlated reversal whereas sample $P1$ shows an extended switching field distribution. The $P2$ results are somewhat surprising and indicate that the CoO layer provides an excellent seed layer for the growth of high-quality Co/Pt multilayers.

Shown in Figs. 1(d)–1(f) are the corresponding room temperature MFM images. The images were acquired after the samples were demagnetized. Consistent with the magnetization results there are clear differences in the domain

structure. For the longitudinal sample [Fig. 1(d)] there is low magnetic contrast arising from the in-plane magnetic variations and domain structure. The low contrast is expected since the MFM is sensitive to stray fields outside the film which tends to be low for in-plane magnetized samples. There is much stronger magnetic contrast for the perpendicular magnetized samples. Sample $P1$ [Fig. 1(e)] has small more disordered magnetic domains suggesting a more disordered multilayer structure. Sample $P2$ has significantly larger domain, consistent with expectations for a thin film with perpendicular anisotropy and little domain wall pinning. In such films the characteristic width of the domains is determined from a balance between the domain wall and dipolar energies and varies with the film thickness.[20] There is about a factor of 5 difference in the domain size comparing sample $P1$ and $P2$ although the two structures are nominally the same structures. Although sample $P1$ has a slightly thicker Co layer next to the CoO layers than $P2$ as reflected in the lower remanent magnetization, the main differences in the domains reflect different microstructural properties of the two samples.

B. Low temperature

The samples were field cooled to low temperatures in applied cooling fields ranging from well below H_{ex} to well above. At low temperatures the CoO layer orders in the presence of the thinner FM layer and, thus, biases this layer. The coercivity of the thinner layers were >5 kOe at 50 K so measurements with fields <5 kOe measure primarily the response of the thicker FM layer. When cooled in an applied field $H<H_{ex}$, the two ferromagnetic layers are antiparallel and the thinner layer is biased opposite to the cooling field direction. For cooling fields $H>H_{ex}$ the ferromagnetic layers are parallel and the thinner layer is biased in the same direction as the cooling field. Measuring minor loops of the thicker ferromagnetic layer with increasing cooling field we should observe a reversal of the effective bias acting on the thicker ferromagnetic layer mediated via the Ru layer

Shown in Figs. 2(a), 3(a), and 4 are minor loops of the thicker ferromagnetic layers measured for cooling fields below, above and near the exchange field. We have subtracted the contribution of the thinner pinned FM layers assuming that it is constant with field and then normalized the minor loops. As expected, for small cooling fields [$<H_{ex}$, open symbols in Figs. 2(a), 3(a), and 4] the thicker layer is negatively biased. For large cooling fields ($>H_{ex}$, closed symbols) the thicker FM layer becomes positively biased. The transition from negative to positive bias depends on the interlayer exchange coupling and is determined by $H_{ex}=J_{ex}/M_S t$. The magnitudes of the negative and positive bias values H_{EB} are equal and are determined by $H_{EB}=J_{ex}/M_{S'}t'$ where $M_{S'}$ and t' are the magnetization and thickness of the thicker FM layer. Such behavior is expected from simple exchange-bias models[1] and was also observed for the double superlattice structures.[8] Also, the shapes of the negative and positive biased loops are nearly identical. Increasing the Ru thickness results in the change in sign of J_{ex} such that the thin and thick layer are ferromagnetically coupled. For such a structure, we observe only negative bias, independent of the cooling field.

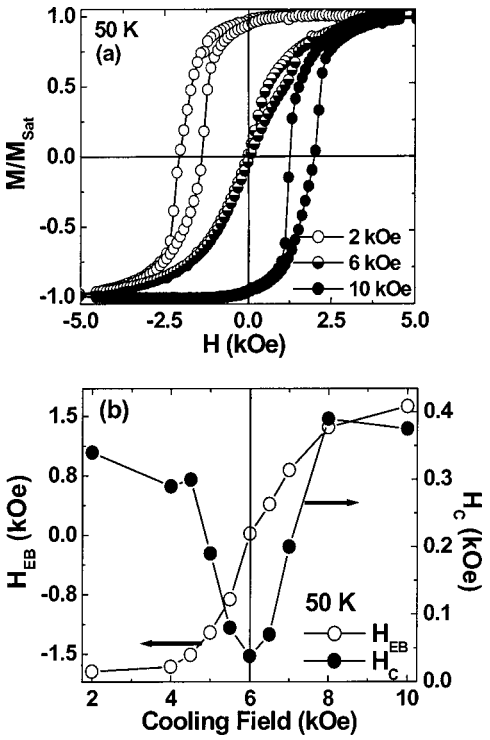

FIG. 2. 50-K magnetization results for the longitudinally magnetized Co(40 Å)/Ru(9 Å)/Co (16 Å)/CoO (~10 Å) sample. (a) shows ±5-kOe minor loops of the thicker FM layer measured after field cooling in applied fields of 2, 6, and 10 kOe. The minor loops were normalized after the contribution of the thinner pinned FM layer was subtracted. (b) The value of the exchange bias H_{EB} and coercivity H_C of the minor loops for various cooling fields. The vertical line indicates the cooling field where the effective bias switches from negative to positive.

The negative and positive bias behavior is similar in all the samples and roughly independent of the anisotropy and disorder and depending only on the interlayer exchange coupling and the thickness of the FM layers. However, the samples show marked differences in the transition region between negative and positive bias. This can be seen in the loops when cooled in an applied field near H_{ex}. For all cases the effective bias is near zero but the shape of the loop changes dramatically. For the longitudinal sample (Fig. 2), the minor loop has zero coercivity and resembles a hard-axis loop. For perpendicular sample $P1$ (Fig. 3), the minor loop is symmetric about $H=0$ but the coercivity is enhanced. Perpendicular sample $P2$ (Fig. 4) exhibits a bifurcated loop where either negative or positive biased regions coexist in the sample. Such bifurcated loops are similar to that observed in Refs. 21 and 22 for zero-field cooled samples in different domain states.

Figures 2(b) and 3(b) show the bias field (i.e., center of the minor loop) and coercivity of the minor loop versus cooling field for the longitudinal sample and sample $P1$, respectively. For both samples the exchange bias gradually changes from negative to positive as the cooling field increases. However, the coercivity goes through a minimum at the point

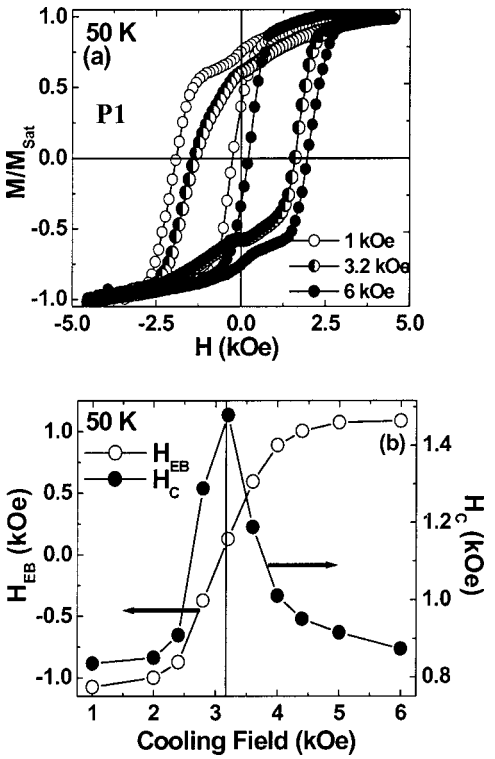

FIG. 3. 50-K magnetization results for perpendicularly magnetized sample $P1$: $[\mathrm{Pt}(7\ \text{Å})/\mathrm{Co}(4\ \text{Å})]_{10}/\mathrm{Ru}(9\ \text{Å})/[\mathrm{Co}(4\ \text{Å})/\mathrm{Pt}(7\ \text{Å})]_3/\mathrm{Co}(10\ \text{Å})/\mathrm{CoO}(10\ \text{Å})$. (a) shows ±5-kOe minor loops of the thicker FM layer measured after field cooling in applied fields of 1, 3.2, and 6 kOe. The minor loops were normalized after the contribution of the thinner pinned FM layer was subtracted. (b) The value of the exchange bias H_{EB} and coercivity H_C of the minor loops for various cooling fields. The vertical line indicates the cooling field where the effective bias switches from negative to positive.

where H_{EB} crosses zero for the longitudinal sample while for sample $P1$ the coercivity reaches a maximum when H_{EB} equals zero. The coercivity increased by 750 Oe when the measured $H_{\mathrm{EB}}=0$. This magnitude of coercivity enhancement is ~70% of maximum H_{EB} value.

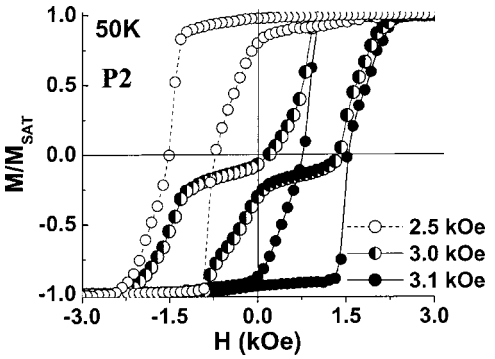

FIG. 4. 50-K magnetization results for perpendicularly magnetized sample $P2$: $\mathrm{CoO}(10\ \text{Å})/[\mathrm{Co}(4\ \text{Å})/\mathrm{Pt}(7\ \text{Å})]_2/\mathrm{Co}(4\ \text{Å})/\mathrm{Ru}(9\ \text{Å})/[\mathrm{Co}(4\ \text{Å})/\mathrm{Pt}(7\ \text{Å})]_{10}$. (a) shows ±3-kOe minor loops of the thicker FM layer measured after field cooling in applied fields of 2.5, 3.0, and 3.1 kOe. The minor loops were normalized after the contribution of the thinner pinned FM layer was subtracted.

IV. DISCUSSION AND CONCLUSIONS

The origin of these different behaviors can be related to differences in the anisotropy and disorder of the samples. For the longitudinal sample, the Co films are polycrystalline and isotropic in plane. Therefore we expect the thinner FM layer to rotate away from the field direction in a spin-flop configuration as H approaches H_{ex}.[19] At the cooling field $H\sim H_{\mathrm{ex}}$ the thinner Co layer will be roughly perpendicular to the field direction. When cooled at this field value, the thinner Co layer will be biased by the CoO layer and is set orthogonal to the cooling field direction. Therefore the bias field at low temperatures that is mediated by the Ru interlayer and acting on the thicker FM layer will be orthogonal to the applied field. This transverse bias field results in the observed hard-axis behavior and suppression of coercivity for this sample. The magnitude of the induced anisotropy field estimated from the field required to saturate the hard-axis loops equals the maximum bias value, as expected, since they both arise from interlayer exchange interaction.

For the perpendicularly biased samples $P1$ and $P2$, the FM layers have uniaxial anisotropy and the spin-flop configuration will be suppressed at $H=H_{\mathrm{ex}}$ in favor of a reversal mechanism dominated by domain nucleation and propagation. As the magnitude of the cooling field approaches H_{ex} reverse domains form in the thinner FM layer where $H=H_{\mathrm{ex}}$ corresponds the equal population of up and down domains. Field cooling in this configuration results in the thinner FM domain structure being frozen into the CoO. Thus, the thicker FM layer becomes locally either positively or negatively biased. The response of the FM layer will depend on the length scale of the variations in the local biasing. If these regions are large compared to the characteristic reverse domain size in the thicker FM layer, then the film will reverse locally in biased regions and a bifurcated loop similar to that observed in Fig. 4 is expected. This is consistent with the image in Fig. 1(e) that shows large domains in the thicker FM layer.

If the regions of local biasing are comparable to reverse domains of the FM layer, the local regions add magnetic disorder that limits the expansion of reverse domains and enhances the coercivity. This behavior is observed for sample $P1$ [Figs. 1(b), 1(d), and 3] and is qualitatively similar to that posited to explain the behavior of the $\mathrm{MnF_2}/\mathrm{Fe}$ bilayers in Ref. 15. In this reference the expected coercivity enhancement is given by

$$\Delta H_C = J_{\text{AFM-FM}} L / d_{\text{AFM}} M_{S'} t' . \tag{1}$$

where $J_{\text{AFM-FM}}$ is the exchange energy between the FM and AFM layers, L is the domain wall length propagating in the FM layer during reversal, d_{AFM} is the characteristic domain size in the AFM pinning layer and $M_{S'}$ and t' are the magnetization and thickness of the FM layer, respectively. For our case, $J_{\text{AFM-FM}}/M_{S'}t'$ equals the maximum value of H_{EB} and Eq. (1) reduces to $\Delta H_C = H_{\mathrm{EB}} L/d_{\text{AFM}}$ where d_{AFM} is set by the size of the domains in the thinner FM layer when the cooling field $H=H_{\mathrm{ex}}$. Unfortunately, we do not have a direct measure of this length scale. The images in Fig. 1 are measured in the remanent state and correspond to domains in the

antiferromagnetically coupled layers. The domains in the thinner layer in an applied field are expected to be different. However, by comparing Fig. 1(d) with 1(e) we can conclude that the domains in sample $P1$ are significantly smaller than those in sample $P2$. Within this model we can estimate the characteristic reverse domain size of the FM layer to that of the biasing layer. We find these two length scales are comparable because the coercivity enhancement is ~70% of the measured exchange bias. This result gives strong support for the ideas discussed in Ref. 15 that local variation in the bias explains the observed coercivity enhancement. In addition, this study points out that qualitatively different coercivity behavior may be expected if the domain size in the AFM layer is increased or for systems with lower or random anisotropy in the AFM layer.

In conclusion, we have described the magnetic response of antiferromagnetically coupled Co/Ru/Co trilayers and $[\mathrm{Co/Pt}]_N/\mathrm{Co/Ru/}[\mathrm{Co/Pt}]_M$ multilayers where the thinner FM layer is exchange biased by a CoO layer. We use these structures as a model system for studying positive exchange bias. The current models relate positive bias to a competition between the Zeeman energy of the cooling field acting on the surface spins of the antiferromagnet and the antiferromagnetic coupling between the FM and AFM layer.[12,17] By adding a thin FM layer to the top of the AFM layer to mimic the surface spins and then antiferromagnetically coupling it to a thicker FM layer, both the Zeeman energy and the interlayer coupling can be controlled and quantified. We find the expected transition from negative to positive bias with increased cooling field. We also observe three distinct hysteresis loop behaviors in the transition region between positive and negative bias that can be related to differences in the microstructure and anisotropy of the constituent layers.

ACKNOWLEDGMENTS

The authors would like to acknowledge helpful discussions with Chris Leighton. O.H. was partially supported by the Deutsche Forschungsgemeinschaft via a Forschungsstipendium under Contract No. HE 3286/2-1.

[1] W. P. Meiklejohn and C. P. Bean, Phys. Rev. **102**, 1413 (1956); **105**, 904 (1957).
[2] J. Nogués and I. K. Schuller, J. Magn. Magn. Mater. **192**, 203 (1999).
[3] A. E. Berkowitz and K. Takano, J. Magn. Magn. Mater. **200**, 552 (1999).
[4] J. C. S. Kools, IEEE Trans. Magn. **32**, 3165 (1996).
[5] B. Dieny, V. S. Speriosu, S. S. P. Parkin, B. A. Gurney, D. R. Wilhoit, and D. Mauri, Phys. Rev. B **43**, 1297 (1991).
[6] M. Kiwi, J. Magn. Magn. Mater. **234**, 584 (2001).
[7] R. L. Stamps, J. Phys. D **33**, R247 (2000).
[8] J. S. Jiang, G. P. Felcher, A. Inomata, R. Goyette, C. Nelson, and S. D. Bader, Phys. Rev. B **61**, 9653 (2000).
[9] S. G. E. te Velthuis, J. S. Jiang, and G. P. Felcher, Appl. Phys. Lett. **77**, 2222 (2000).
[10] L. Lazar, J. S. Jiang, G. P. Felcher, A. Inomata, S. D. Bader, J. Magn. Magn. Mater. **223**, 299 (2001).
[11] J. Nogués, D. Lederman, T. J. Moran, and I. K. Schuller, Phys. Rev. Lett. **76**, 4624 (1996).
[12] C. Leighton, J. Nogués, H. Suhl, and I. K. Schuller, Phys. Rev. B **60**, 12 837 (1999).
[13] J. Nogués, C. Leighton, and I. K. Schuller, Phys. Rev. B **61**, 1315 (2000).
[14] M. J. Pechan, D. Bennett, N. Teng, C. Leighton, J. Nogués, and I. K. Schuller, Phys. Rev. B **65**, 064410 (2002).
[15] C. Leighton, J. Nogués, B. J. Jönsson-Åkerman, and I. K. Schuller, Phys. Rev. Lett. **84**, 3466 (2000).
[16] M. Kiwi, J. Mejía-López, R. D. Portugal, and R. Ramírez, Solid State Commun. **116**, 315 (2000).
[17] F. Canet, S. Mangin, C. Bellouard, and M. Piecuch, Europhys. Lett. **52**, 594 (2000).
[18] S. Maat, K. Takano, S. S. P. Parkin, and E. E. Fullerton, Phys. Rev. Lett. **87**, 087202 (2001).
[19] W. Folkerts and S. T. Purcell, J. Magn. Magn. Mater. **111**, 306 (1992).
[20] G. Bochi, H. J. Hug, D. I. Paul, B. Stiefel, A. Moser, I. Parashikov, H.-J. Guntherodt, and R. C. O'Handley, Phys. Rev. Lett. **75**, 1839 (1995).
[21] P. Miltényi, M. Gierlings, M. Bamming, U. May, G. Güntherodt, J. Nogués, M. Gruyters, C. Leighton, and I. K. Schuller, Appl. Phys. Lett. **75**, 2304 (1999).
[22] N. J. Gökemeijer, J. W. Cai, and C. L. Chien, Phys. Rev. B **60**, 3033 (1999).